Smooth Switching Hinf PI Controller for Local Traffic On-ramp Metering, an LMI Approach

Antoine Lemarchand, John Jairo Martinez Molina, Damien Koenig

Smooth Switching H_∞ PI Controller for Local Traffic On-ramp Metering, an LMI Approach

Antoine Lemarchand * **John J. Martinez** * **Damien Koenig** *

* *Control system department, GIPSA-lab, UMR 5216, Grenoble-INP, France.*

Abstract: This paper deals with the design of robust H_∞ PI controllers for traffic control. The uncertain Cell Transmission Model (CTM) used in this article is a switched affine uncertain system. A robust PI controller is calculated for each mode of the CTM. Since the switching law contains uncertainties there is chattering issues at switching surface. To deal with this problem, we propose to use a smooth switching rule. The smooth switching is realized applying a convex combination of controllers on the system. The choice of the convex combination is motivated by a statistical analysis of experimental data. The global stability of the closed loop system is proven by computing a PieceWise Quadratic (PWQ) Lyapunov function. A LMI is given to calculate the controllers. The approach is illustrated and validated in a study-case simulation.

Keywords: Traffic control, switching theory, uncertain linear systems

1. INTRODUCTION

The amount of vehicles on roads increases every day, and causes a waste of time and money (Schrank and Lomax [2007]). With the construction of new roads, traffic control via on-ramp metering is one of the most explored ways to deal with this problem. The on-ramp metering aims at the improving of traffic condition by controlling the inflow of freeways.

Most of the solution proposed are based on a hierarchical control scheme (Stephanedes and Chang [1993],Kotsialos and Papageorgiou [2005]). This architecture is constituted by the high level (optimization layer) and by the low level (local controller level).

The high level layer computes the optimal references (concentrations) to be tracked by the system. This layer is usually based on linear programming algorithms (Jacquet [2008],Jacquet et al. [2008],Gomes and Horowitz [2006]). These references are open loop calculation based on a nominal model. Due to parametric uncertainties and disturbances, the optimal solution computed by this algorithm can't be applied directly on the system.

Therefore, we use the low level layer to ensure that the system really tracks optimal references. In this layer, references are locally applied to on-ramps neighborhoods as shown in Figure 1. Several approaches have been explored to solve this issue such as ALINEA (Haj-Salem et al. [2001]), and others such as (Sun and Horowitz [2005],Sun and Horowitz [2006]). In this article, we focus on the local regulation layer. We assume that the optimal trajectories computed by the optimization layer are known. The parameters of the model are strongly uncertain. The Cell Transmission Model (CTM) can be extended with a model of uncertainties (Lemarchand et al. [2010b])(Lemarchand et al. [2010a]). This model is presented in the form of a uncertain state dependant switching system. Thanks to this model, a bank of robust switched PI controller can be designed (Lemarchand et al. [2010a]). These PI controllers guarantee the attenuation of the H_∞ norm of the transfer function between disturbance and tracking error. Since the switching rules contain uncertain parameters, the switching sequence cannot be obtained directly from the measurements. We propose to use probability functions to deal with this problem. With this formulation, the problem is similar to a Takagi-Sugeno model (Johansson et al. [1999],Feng [2003]).

The paper is organized as follows. A brief presentation of the uncertain CTM is provided in Section 2. Section 3 presents the study case. Section 4 presents the state space partition, and the associated probability functions. Section 5 presents the design of robust switched PI controller. The stability of the closed loop system is proved with a PieceWise Quadratic (PWQ) Lyapunov function. The H_∞ controllers are calculated by solving a LMI optimization problem. Some simulation results are provided in Section 6. In Section 7, some concluding remarks end the paper.

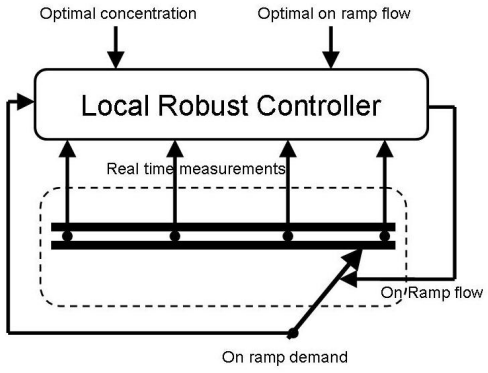

Fig. 1. Local regulation.

2. UNCERTAIN CTM

The CTM is a discrete first order traffic model. It considers the road section divided into elementary cells. In each cell, the density of vehicles $\rho(k)$ is considered homogenous. The CTM is constituted of cells, junctions, on-ramps and off-ramps. These elements are depicted in Figure 2. The CTM is characterized by an equation of conservation for vehicles and an equation of flow calculation.

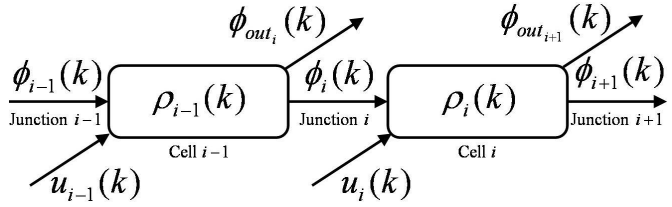

Fig. 2. Cell Transmission Model.

2.1 Conservation Equation

For each cells,

$$\rho_i(k+1)=\rho_i(k)+\frac{T}{l_i}(\phi_i(k)+u_i(k)-\phi_{i+1}(k)-\phi_{out_{i+1}}(k)), \quad (1)$$

where $\rho_i(k)$ (veh/km) is the density of vehicles in cell i, $\phi_i(k)$ and $\phi_{i+1}(k)$ (veh/h) are respectively the flow in junction i and $i+1$, $u_i(k)$ and $\phi_{out_{i+1}}(k)$ (veh/h) are respectively the flow entering and leaving cell i via on/off-ramps, l_i is the length of cell i and T is the period of discretized time.
To guarantee numerical stability, we must choose the length of cells such that : $l_i < T.v_i, \forall i = 1, ..., N$ (N, the number of cells).

2.2 Flow Calculation

The flow between two cells is the minimum of three quantities (C. F. Daganzo [1995]).

$$\phi_i(k) = min(v_{i-1}.\rho_{i-1}(k) - \phi_{out_{i+1}}(k), \phi_{M_i}, w_i.(\rho_{J_i} - \rho_i(k)) - u_i(k)). \quad (2)$$

with $v_i, (km/h)$ the free flow speed, $w_i(km/h)$ the backward congestion propagation speed, $\rho_{J_i}, (veh/km)$ the jam density (i.e. maximal density), and $\phi_{M_i}, (veh/h)$ the maximum flow that can travel from upstream to downstream cell.

Junction modes:
From(2) one can identify the three possible modes of the junction: A *free* mode (F) where the flow is proportional to the upstream cell concentration, a *decoupled* mode (D) where the flow is equal to the maximal flow, and a *congested* mode (C) where the flow is proportional to the remaining space in downstream cell. A graphical representation of (2) is provided in Figure 3. It is called the fundamental diagram. This kind of diagram appears in every traffic issues using macroscopic model (Geroliminis and Daganzo [2008]).

2.3 Uncertain Fundamental Diagram

The nominal parameters of the fundamental diagram can be computed using the calibration methods described in Munoz et al. [2004] with experimental datas [1] . The obtain diagram contains strong uncertainties. They can be modeled as the following parametric uncertainties (Lemarchand et al. [2010a]):

$$\begin{aligned} v_{i-1}(k) &= v_{0_{i-1}} + \Delta v_{i-1}(k), \\ \phi_{M_i}(k) &= \phi_{M_{0_i}} + \Delta\phi_{M_i}(k), \\ w_i(k) &= w_{0_i} + \Delta w_i(k), \end{aligned} \quad (3)$$

where v_0, ϕ_{M_0} and w_0 are respectively the nominal free flow speed, maximum flow, and backward congestion propagation speed computed thanks to (Munoz et al. [2004]), and Δv, $\Delta\phi_M$ and Δw the corresponding uncertainties. The uncertain fundamental diagram is depicted in Figure 3.

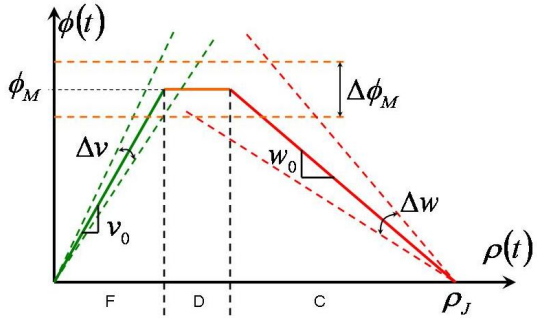

Fig. 3. Fundamental diagram with parametric uncertainties.

2.4 Compact Matrix Form

For a given section of road, the CTM can be written as a discrete uncertain linear switched system (Lemarchand et al. [2010a]). Define

$$\alpha(k) := [\alpha_1(k), \cdots, \alpha_{N+1}(k)] \quad (4)$$

where $\alpha_i(k) \in \{F, D, C\}$ represents the mode of junction i.
For all $\alpha(k)$ the dynamics of a freeway section can be written as an uncertain dynamical system:

$$\begin{aligned} \rho(k+1) = \quad & (A_{0_{\alpha(k)}} + F_{\alpha(k)}\Delta(k)G).\rho(k) \\ & + a_{\alpha(k)} + B_{\alpha(k)}.u(k) + E_{\alpha(k)}.d(k) \end{aligned} \quad (5)$$

$$\Delta(k)^T\Delta(k) < 1 \quad (6)$$

where $\rho(k) = [\rho_1(k), ..., \rho_N(k)]$ is the state vector of vehicle densities for each cell, $a_{\alpha(k)}$ a constant, $u(k)$ the on ramp controlled flows and $d(k)$ a vector of external disturbances. $A_{0_{\alpha(k)}}, B_{\alpha(k)}, E_{\alpha(k)}, F_{\alpha(k)}, G$ are know matrices of appropriate dimensions. Each matrices and vectors are defined in (Lemarchand et al. [2010a]).

3. STUDY CASE

In this article, we consider the neighborhood depicted in Figure 4. We consider here that in normal traffic condition (i.e. without accidents) the different mode of the section that can occurs are the following:

- case 1 : $\alpha(k) = [FFFFFF]$

[1] Real time measurements realized on D383 road (near Lyon, France) provided by DDE69

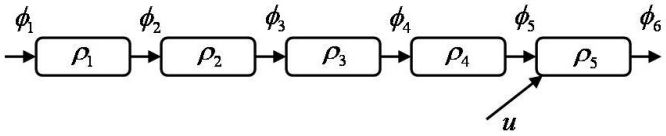

Fig. 4. On-ramp neighborhood.

- case 2 : $\alpha(k) = [FFFFFD]$
- case 3 : $\alpha(k) = [FFFFCD]$
- case 4 : $\alpha(k) = [FFFCCD]$
- case 5 : $\alpha(k) = [FFCCCD]$
- case 6 : $\alpha(k) = [FCCCCD]$

where $\alpha(k)$ is defined by (4).We notate Ω the set of cases. In case 1, all the junctions of the section are in *free* mode (F). Just before congestion appears (case 2) junction 4 switches to *decoupled* mode (D). Then in case 3, 4, 5 and 6, the congestion propagates backward (i.e. junction 5 to 2 switch to *congested* mode (C)).

4. PROBABILITY FUNCTIONS

Since there are uncertain parameters on the switching rules, $\alpha(k)$ can't be obtained directly from $\rho(k)$. Consider a junction without off/on-ramps. We take the following notations:

$$\begin{aligned} v_{M_i} &= v_{0_i} + \|\Delta v_i\|_\infty \\ v_{m_i} &= v_{0_i} - \|\Delta v_i\|_\infty \\ w_{M_i} &= w_{0_i} + \|\Delta w_i\|_\infty \\ w_{m_i} &= w_{0_i} - \|\Delta w_i\|_\infty \end{aligned} \tag{7}$$

Then, from (2) junction i is *free* if

$$v_{M_{i-1}}\rho_{i-1}(k) \leq w_{m_i}(\rho_{J_i} - \rho_i(k)), \tag{8}$$

congested if

$$v_{m_{i-1}}\rho_{i-1}(k) \geq w_{M_i}(\rho_{J_i} - \rho_i(k)) \tag{9}$$

On the partition of state space where both (8) and (9) are false, the mode of junction i depends on uncertainties. From their we deduce the subspace where junction i is

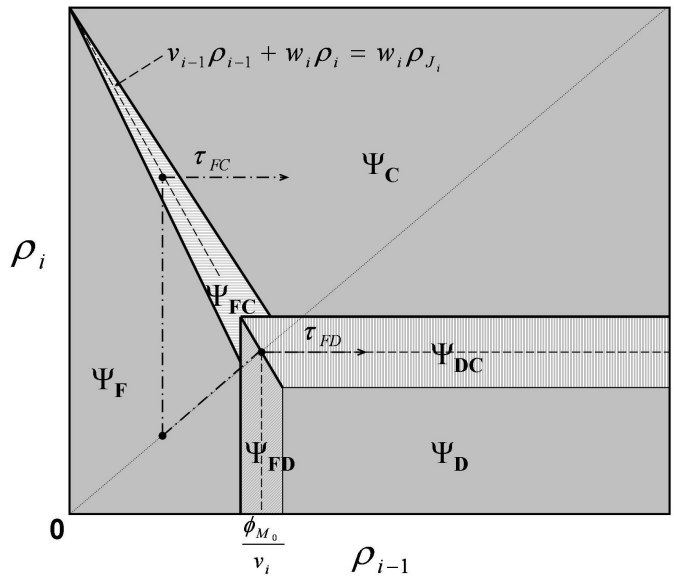

Fig. 5. Mode subspaces for junction i.

in *free* mode (Ψ_{F_i}), in *congested* mode (Ψ_{C_i}) in *decoupled* mode (Ψ_{D_i}), either *free* or *congested* mode (Ψ_{FC_i}), either *free* or *decoupled* mode (Ψ_{FD_i}), either decoupled or *congested* mode (Ψ_{DC_i}). These subspace are depicted in Figure 5. We perform a statistical study of experimental data to characterize the sub space Ψ_{FC_i}. The normalized probability density functions for uncertainties Δv and Δw (defined in equation (3)) obtained are depicted in Figure 6. The probability to be in a specific mode can be computed

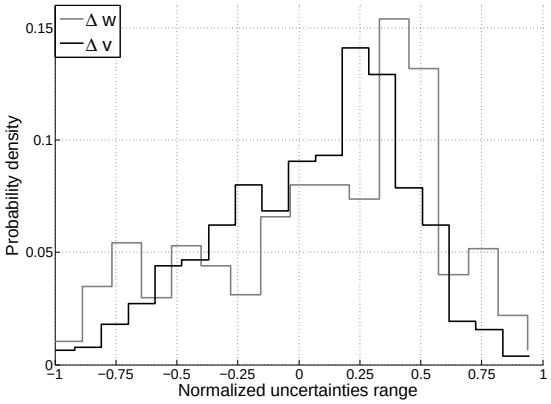

Fig. 6. Normalized probability density function of Δ_v and Δ_w.

from these probability density function, doing a convolution product. We approximate the cumulate probability density by:

$$\mu(x) = \frac{\arctan((\frac{x-a}{b-a} - .5).\beta) + 1}{2 * \arctan(\beta/2)} \tag{10}$$

where a and b are the bound calculated thanks to (8) and (9), and β a tuning parameter. The comparison between the normalized cumulate convolution product and the approximate function (11) is given in Figure 7.

The probability for junction i to be in *free*, *decoupled* or *congested* mode are respectively denoted $\mu_{F_i}(\rho), \mu_{D_i}(\rho), \mu_{C_i}(\rho)$. From (8),(9) and (11) we write:

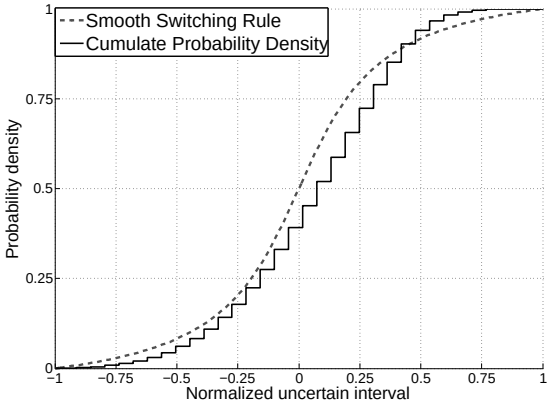

Fig. 7. Normalized cumulate convolution product, approximation function ($\beta = 8, a = -1, b = 1$).

$$\mu_{C_i}(\rho) = \begin{cases} 0, if \rho_i < \rho_{m_{i-1}} \\ 1, if \rho_i > \rho_{M_{i-1}} \\ \dfrac{\arctan((\frac{\rho_i - \rho_{m_{i-1}}}{\rho_{M_{i-1}} - \rho_{m_{i-1}}} - .5).\beta) + 1}{2 * \arctan(\beta/2)}, \text{otherwise} \end{cases} \quad (11)$$

$$\rho_{m_{i-1}} = \frac{w_{m_i}}{v_{M_{i-1}}}(\rho_{J_i} - \rho_i(k)) \quad (12)$$

$$\rho_{M_{i-1}} = \frac{w_{M_i}}{v_{m_{i-1}}}(\rho_{J_i} - \rho_i(k)) \quad (13)$$

Figure 8 depicts $\mu_F(\rho)$ $\mu_C(\rho)$. From their, we can build

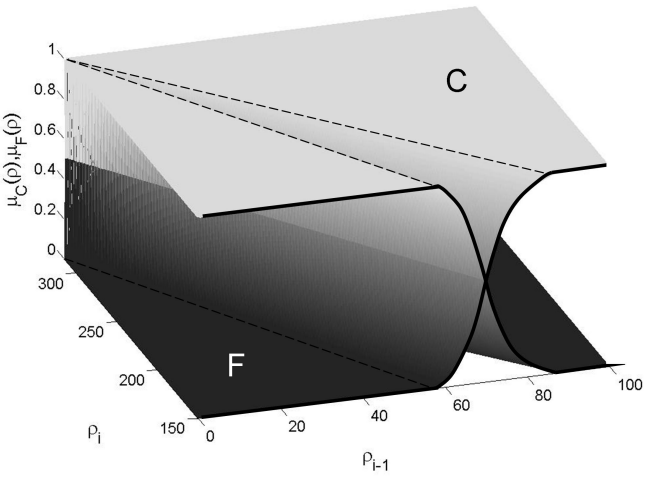

Fig. 8. Probability functions, $\mu_{F_i}(\rho), \mu_{C_i}(\rho)$.

the subspaces for each case as an intersection of the subspaces defined in Figure 5. We define Ψ_{Case3} as the subspace where the subsystem 3 is active, Ψ_{Case4} as the subspace where the subsystem 4 is active and $\Psi_{Case3,4}$ as the subspace where the subsystem 3 or 4 may be active. They are defined as follows :

$$\begin{array}{rcl} \Psi_{Case3} & = & \Psi_{F_1} \cap \Psi_{F_2} \cap \Psi_{F_3} \cap \Psi_{F_4} \cap \Psi_{C_5} \cap \Psi_{D_6} \\ \Psi_{Case4} & = & \Psi_{F_1} \cap \Psi_{F_2} \cap \Psi_{F_3} \cap \Psi_{C_4} \cap \Psi_{C_5} \cap \Psi_{D_6} \\ \Psi_{Case3,4} & = & \Psi_{F_1} \cap \Psi_{F_2} \cap \Psi_{F_3} \cap \Psi_{FC_4} \cap \Psi_{C_5} \cap \Psi_{D_6} \end{array} \quad (14)$$

We notate I the set of subspaces. I_0 is the set of partitions containing the origin, $I_1 = I \backslash I_1$. We notate $\kappa(\Psi_i)$ the set of subsystem that may be active in subspace Ψ_i. The probability to be in Case n is called $\mu_n(\rho)$. It can be easily define as a product of corresponding individual probabilities for each junctions. Remark that:

$$\mu_n(\rho) = 0, \rho \in \Psi_i, n \notin \kappa(\Psi_i) \quad (15)$$

$$\mu_n(\rho) \neq 0, \rho \in \Psi_i, n \in \kappa(\Psi_i) \quad (16)$$

$$\sum_{n \in \kappa(\Psi_i)} \mu_n(\rho) = 1 \quad (17)$$

5. REGULATOR DESIGN

We propose to design a smooth switching PI controller. A PI controller is designed for each case of Ω. Then a convex combination of these PI controllers is applied on the system. The convex combination is calculated with the probabilities defined in the previous section. To design the controllers that ensure the attenuation of disturbances, the system has to be extended with an integrator (Section 5.1). To ensure stability of the closed loop system, we have to compute a PWQ Lyapunov function (Section 5.2). The final LMI formulation with the H_∞ attenuation criteria is presented in Section 5.3.

5.1 Extended system

We extend our system with an integrator. To keep the stabilizability property of the system, we can only extend one state of the system with an integrator. For the case 1 and 2, we choose to extend the system with an integrator on $\epsilon_5(k)$ (where $\epsilon_5(k) = \rho_5(k) - \rho_5^*(k)$) . For the case 3 to 6, we choose to extend the system with an integrator on the density of the cell where the congestion front stand (respectively $\epsilon_4(k)$ to $\epsilon_1(k)$). So, the new state vector becomes

$$X(k) = \begin{pmatrix} \rho(k) \\ z(k) \end{pmatrix} \quad (18)$$

with:

$$z(k+1) = z(k) + \begin{cases} \epsilon_5(k) & \text{, if case 1 or 2} \\ \epsilon_4(k) & \text{, if case 3} \\ \epsilon_3(k) & \text{, if case 4} \\ \epsilon_2(k) & \text{, if case 5} \\ \epsilon_1(k) & \text{, if case 6} \end{cases} \quad (19)$$

The extended system is described in a compact form as follows:

$$\begin{cases} X(k+1) = & (A_{a_{\alpha(k)}} + F_{a_{\alpha(k)}}.\Delta(k).G_a).X(k) \\ & + a_{\alpha(k)} + B_{a_{\alpha(k)}}.u(k) + E_{a_{\alpha(k)}}.w(k) \\ Z(k) = & C_{a_{\alpha(k)}}.X(k) \end{cases} \quad (20)$$

where $Z(k)$ is the tracking error of the cell where congestion front stands.
For convenient notation, we also introduce:

$$\bar{A}_{a_{\alpha(k)}} = \begin{pmatrix} A_{a_{\alpha(k)}} & a_{\alpha(k)} \\ 0 & 0 \end{pmatrix}$$

$$\bar{F}_{a_{\alpha(k)}} = \begin{pmatrix} F_{a_{\alpha(k)}} \\ 0 \end{pmatrix}$$

$$\bar{G}_a = (G_a \ 0)$$

$$\bar{B}_{a_{\alpha(k)}} = \begin{pmatrix} B_{a_{\alpha(k)}} \\ 0 \end{pmatrix}$$

$$\bar{E}_{a_{\alpha(k)}} = \begin{pmatrix} E_{a_{\alpha(k)}} \\ 0 \end{pmatrix}$$

$$\bar{C}_{a_{\alpha(k)}} = \begin{pmatrix} C_{a_{\alpha(k)}} & 0 \end{pmatrix}$$

$$\bar{X}(k) = \begin{pmatrix} X(k) \\ 1 \end{pmatrix}$$

5.2 PWQ Lyapunov Function

To ensure that the system is globally stable, we have to find a candidate lyapunov function. Since a global Lyapunov function can't be found, we build a piecewise quadratic Lyapunov function. On this purpose, we have to ensure continuity at each bound of subspaces defined in (14). These bounds are represented in continuous lines in Figure 5.

(Johansson and Rantzer [1998]) proposes the following approach.

Proposition 1. Choose a candidate Lyapunov function of the form:

$$V(X) = \begin{cases} X^T P_{\Psi_i} X, \ \forall X \in \Psi_i, i \in I_0 \\ \bar{X}^T \bar{P}_{\Psi_i} \bar{X}, \ \forall X \in \Psi_i, i \in I_1 \end{cases} \quad (21)$$

with I_0 the set of partitions containing the origin, $I_1 = I \backslash I_0$ and where P_i is chosen as follows:

$$P_{\Psi_i} = \begin{cases} L_i^T T L_i, \ \forall X \in \Psi_i, i \in I_0 \\ \bar{L}_i^T T \bar{L}_i, \ \forall X \in \Psi_i, i \in I_1 \end{cases} \quad (22)$$

If

$$\bar{L}_i \bar{X} = \bar{L}_j \bar{X}, \forall X \in \Psi_i \cap \Psi_j, i, j \in I \quad (23)$$

$$\bar{L}_i = \begin{pmatrix} L_i \\ 0 \cdots 0 \end{pmatrix}, \qquad \forall i \in I_0 \quad (24)$$

Then $V(X)$ is continuous along all bounds of the partitioned state space.

The problem is now to compute matrices $\bar{L}_i, i \in I$. An efficient approach to compute theses matrices is presented in (Johansson et al. [2000]).

According to Figure 5, the partitioned state space for a junction contains 7 bounds. Depending of the junction characteristics, some of these bounds may not cet crossed. Ensuring the continuity at each bounds may be conservative and may increase the problem size.

First, we consider a junction with no on/off-ramps, the system can only cross 2 bounds ($\Psi_{Fi} \cap \Psi_{FCi}$ and $\Psi_{FCi} \cap \Psi_{Ci}$). A typical trajectory of the system in this case (τ_{FC}) is represented in Figure 5. We start by computing $\bar{L}1_{\Psi_{Fi}}$ and $\bar{L}1_{\Psi_{FCi}}$ (for junction i) such that

$$\bar{L}1_{\Psi_{Fi}} \begin{pmatrix} \rho_{i-1} \\ \rho_i \\ 1 \end{pmatrix} = \bar{L}1_{\Psi_{FCi}}, \forall \begin{pmatrix} \rho_{i-1} \\ \rho_i \end{pmatrix} \in \Psi_{Fi} \cap \Psi_{FCi} \quad (25)$$

This condition will ensure continuity of the Lyapunov function at the bound $\Psi_{Fi} \cap \Psi_{FCi}$ defined by the equation:

$$v_{M_{i-1}} \rho_{i-1} + w_{m_i} \rho_i = w_{m_i} \rho_{J_i} \quad (26)$$

(see Figure 5). As demonstrated in (Johansson and Rantzer [1998]) the constraint matrices can be computed as

$$\bar{L}1_{\Psi_{Fi}} = \begin{pmatrix} 0 & 0 \\ 0 & I_2 \end{pmatrix} \varepsilon_{\Psi_{Fi}} (\upsilon \varepsilon_{\Psi_{Fi}})^{-1} \begin{pmatrix} C & 0 \\ 0 & 1 \end{pmatrix},$$

$$\bar{L}1_{\Psi_{FCi}} = \begin{pmatrix} 0 & 0 \\ 0 & I_2 \end{pmatrix} \varepsilon_{\Psi_{FCi}} (\upsilon \varepsilon_{\Psi_{FCi}})^{-1} \begin{pmatrix} C & 0 \\ 0 & 1 \end{pmatrix},$$

with

$$\upsilon = \begin{pmatrix} 0 & w_{m_i} \rho_{J_i} & \dfrac{w_{M_i} v_{M_{i-1}}}{v_{m_{i-1}}} \rho_{J_i} \\ 1 & 1 & 1 \end{pmatrix}$$

$$C = (v_{M_{i-1}} \ \ w_{m_i})$$

$$\varepsilon_{\Psi_{Fi}} = \begin{pmatrix} 1 & 0 \\ 0 & 1 \\ 0 & 0 \end{pmatrix}, \varepsilon_{\Psi_{FCi}} = \begin{pmatrix} 0 & 0 \\ 1 & 0 \\ 0 & 1 \end{pmatrix}$$

Using the same procedure, we are able to compute $\bar{L}2_{\Psi_{FCi}}$ and $\bar{L}2_{\Psi_{Ci}}$ such that

$$\bar{L}2_{\Psi_{FCi}} \begin{pmatrix} \rho_{i-1} \\ \rho_i \\ 1 \end{pmatrix} = \bar{L}2_{\Psi_{Ci}}, \forall \begin{pmatrix} \rho_{i-1} \\ \rho_i \end{pmatrix} \in \Psi_{FCi} \cap \Psi_{Ci}. \quad (27)$$

This condition will ensure continuity of the Lyapunov function at the bound $\Psi_{FCi} \cap \Psi_{Ci}$ defined by the equation:

$$v_{m_{i-1}} \rho_{i-1} + w_{M_i} \rho_i = w_{M_i} \rho_{J_i} \quad (28)$$

Then, taking:

$$\bar{L}_{\Psi_{Fi}} = \begin{pmatrix} \bar{L}1_{\Psi_{Fi}} \\ \bar{L}2_{\Psi_{FCi}} \end{pmatrix} \quad (29)$$

$$\bar{L}_{\Psi_{FCi}} = \begin{pmatrix} \bar{L}1_{\Psi_{FCi}} \\ \bar{L}2_{\Psi_{FCi}} \end{pmatrix} \quad (30)$$

$$\bar{L}_{\Psi_{Ci}} = \begin{pmatrix} \bar{L}1_{\Psi_{FCi}} \\ \bar{L}2_{\Psi_{Ci}} \end{pmatrix} \quad (31)$$

(23) holds at all bounds crossed by the system trajectories τ_{FC}.

For a junction containing an on-ramp, the continuity of the Lyapunov function has to be ensured at 3 bounds ($\Psi_{Fi} \cap \Psi_{FDi}$,$\Psi_{FDi} \cap \Psi_{DCi}$,$\Psi_{DCi} \cap \Psi_{Ci}$). Using the previous procedure, we can calculate $\bar{L}_{\Psi_{Fi}}$,$\bar{L}_{\Psi_{FDi}}$,$\bar{L}_{\Psi_{DCi}}$ and $\bar{L}_{\Psi_{Ci}}$ that ensure the continuity of the Lyapunov function.

The constraint matrices for a system with several junctions can be computed as follows:

$$\bar{L}_{\Psi_{Fi} \cap \Psi_{Ci+1}} = \begin{pmatrix} & & 0 \\ & \bar{L}_{\Psi_{Fi}} & \vdots \\ & & 0 \\ 0 & & \\ \vdots & \bar{L}_{\Psi_{Ci+1}} & \\ 0 & & \end{pmatrix} \quad (32)$$

5.3 LMI Formulation

Proposition 2. if $\exists \ T > 0$ and $e_n > 0, U_n, n \in \Omega$ such that:
(33) holds for all $\Psi_i \in I_0, n \in \kappa(\Psi_i)$,
(34) holds for all $\Psi_i \in I_1, n \in \kappa(\Psi_i)$,
The LMI's (33) and (34) are defined at the top of next page.
Then:

- The extended system (20) is stable under state feedback $u(k) = -\sum \mu_n(X(k)) K_n X(k), K_n = U_n T$,
- The H_∞ norm of the transfert function between $w(k)$ and $Z(k)$ is bounded by γ

Proof We write the proof for (33) i.e. for $\Psi_i \in I_0, k \in \kappa(\Psi_i)$. We write the following H_∞ attenuation criteria:

$$\begin{matrix} X(k+1)^T P_{\Psi_i} X(k+1) - X(k)^T P_i X(k) \\ + Z(k)^T Z(k) - \gamma^2 w(k)^T w(k) < 0 \end{matrix} \quad (35)$$

Taking $A_{a_n} - B_{a_n} K_n = \Gamma_n$, (35) is equivalent to

$$\begin{pmatrix} \Pi_{11}^1 & \Pi_{21}^1 \\ * & E_{a_n}^T L_i^T T L_i E_{a_n} - \gamma^2 I \end{pmatrix} < 0 \quad (36)$$

$$\Pi_{11}^1 = (\Gamma_n + F_{a_n}.\Delta(k).G_a)^T L_i^T T L_i (\Gamma_n + F_{a_n}.\Delta(k).G_a) - L_i^T T L_i + C_n^T C_n$$

$$\Pi_{21}^1 = (\Gamma_n + F_{a_n}.\Delta(k).G_a)^T L_i^T T L_i E_{a_n}$$

$$\begin{pmatrix} -T^{-1}L_i^T - L_iT^{-1} + T^{-1} & 0 & T^{-1}A_{a_n}^T L_i^T - U_n^T B_{a_n}^T L_i^T & T^{-1}C_n^T & T^{-1}G_a^T \\ * & -\gamma^2 I & E_{a_n}^T L_i^T & 0 & 0 \\ * & * & -T^{-1} + \epsilon_n L_i F_{a_n} F_{a_n}^T L_k^T & 0 & 0 \\ * & * & * & -I & 0 \\ * & * & * & * & -\epsilon_n I \end{pmatrix} < 0 \quad (33)$$

$$\begin{pmatrix} -T^{-1}\bar{L}_i^T - \bar{L}_iT^{-1} + T^{-1} & 0 & T^{-1}\bar{A}_{a_n}^T \bar{L}_i^T - U_n^T \bar{B}_{a_n}^T \bar{L}_i^T & T^{-1}\bar{C}_n^T & T^{-1}\bar{G}_a^T \\ * & -\gamma^2 I & \bar{E}_{a_n}^T \bar{L}_i^T & 0 & 0 \\ * & * & -T^{-1} + \epsilon_n \bar{L}_i \bar{F}_{a_n} \bar{F}_{a_n}^T \bar{L}_i^T & 0 & 0 \\ * & * & * & -I & 0 \\ * & * & * & * & -\epsilon_n I \end{pmatrix} < 0 \quad (34)$$

Applying Schur complement, we obtain the following inequality:

$$\begin{pmatrix} -L_i^T T L_i + C_n^T C_n & 0 & (\Gamma_i + F_{a_k}.\Delta(k).G_a)^T L_i^T \\ * & -\gamma^2 I & E_{a_n}^T L_i^T \\ * & * & -T^{-1} \end{pmatrix} < 0 \quad (37)$$

Using majoration lemma, (37) holds if $\exists \epsilon_n > 0$ such that:

$$\begin{pmatrix} -L_i^T T L_i + C_n^T C_n & 0 & \Gamma_n^T L_i^T \\ +\epsilon_n^{-1} G_a^T G_a & & \\ * & -\gamma^2 I & E_{a_n}^T L_i^T \\ * & * & -T^{-1} + \epsilon_n L_i F_{a_n} F_{a_n}^T L_i^T \end{pmatrix} < 0 \quad (38)$$

Multiplying on both side by $\begin{pmatrix} T^{-1} & 0 \\ & I \\ 0 & I \end{pmatrix}$ and applying twice Schur complement, the following inequality is obtained:

$$\begin{pmatrix} -T^{-1}L_i^T T L_i T^{-1} & 0 & T^{-1}\Gamma_n^T L_i^T & T^{-1}C_n^T & T^{-1}G_a^T \\ * & -\gamma^2 I & E_{a_n}^T L_i^T & 0 & 0 \\ * & * & \Pi_{33}^2 & 0 & 0 \\ * & * & * & -I & 0 \\ * & * & * & * & -\epsilon_n I \end{pmatrix} < 0 \quad (39)$$

$$\Pi_{33}^2 = -T^{-1} + \epsilon_n L_i F_{a_n} F_{a_n}^T L_i^T$$

Since $-T^{-1}L_i^T T L_i T^{-1} \leq -T^{-1}L_i^T - L_iT^{-1} + T^{-1}$. Then (39) is implied by

$$\begin{pmatrix} -T^{-1}L_i^T - L_iT^{-1} + T^{-1} & 0 & T^{-1}\Gamma_n^T L_i^T & T^{-1}C_n^T & T^{-1}G_a^T \\ * & -\gamma^2 I & E_{a_n}^T L_i^T & 0 & 0 \\ * & * & \Pi_{33}^2 & 0 & 0 \\ * & * & * & -I & 0 \\ * & * & * & * & -\epsilon_n I \end{pmatrix} < 0$$

Taking $U_n = K_n T^{-1}$, LMI (33) is obtained. Then using *Theorem 1* in (Johansson et al. [1999]), the proof is completed. The proof is similar for (34).

6. SIMULATION RESULTS

For simulation, we take the on-ramp neighborhood depicted in Figure 4. We choose the following cell parameters (cells are homogenous):

- Cell length $l = 0.3km$
- Free flow speed $v = 80km/h \pm 5\%$
- Backward congestion speed $v = 35km/h \pm 15\%$
- Maximum flow $\phi_M = 7000km/h \pm 8\%$

These parameters values and uncertainties ranges are chosen according to experimental data.

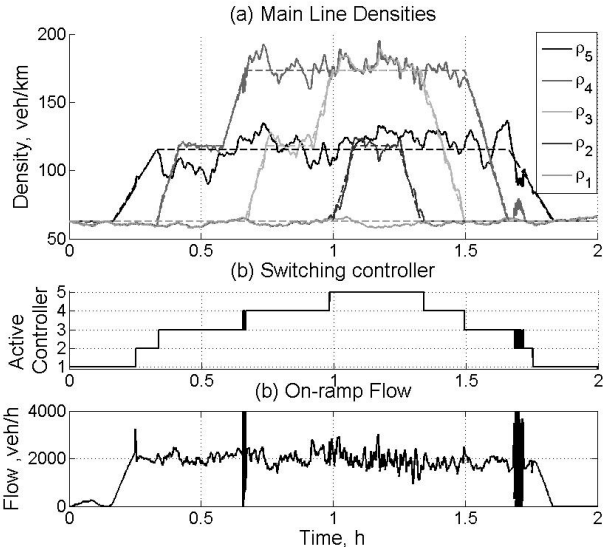

Fig. 9. Switching PI controller

In the scenario we have chosen, the system has to track a congestion front which propagates backward then forward. The system goes from case 1 to case 5 via all the intermediate cases, after that it goes back to case 1. In Figure 9 the controller is chosen according to the nominal switching rule. We can see that the system is following the congestion front despite parametric uncertainties and disturbance. But we can notice that the on-ramp flow is not continuous at switching instant. Moreover some chattering problem appear when system switches from case 3 to case 2 and from case 3 to case 4.

In Figure 10 the controller is calculated as a convex combination. Figure 10(b) represent the obtain convex combination, the dashed lines represent the case calculated with extremum values of the uncertainties (equation (7). We can see that the system still follows the congestion front despite parametric uncertainties and disturbance. Moreover, the continuity of the on-ramp flow is ensured, and there's no switching issues.

7. CONCLUSIONS

In this paper, we have studied a switching system that contains uncertainties in the switching rule. We apply a convex combination of different controllers on the uncertain subspaces. This choice is motivated by a statistical analysis of experimental data. The set of controllers is calculated by LMI resolution. The simulation results show the efficiency of the proposed approach. The LMI condition

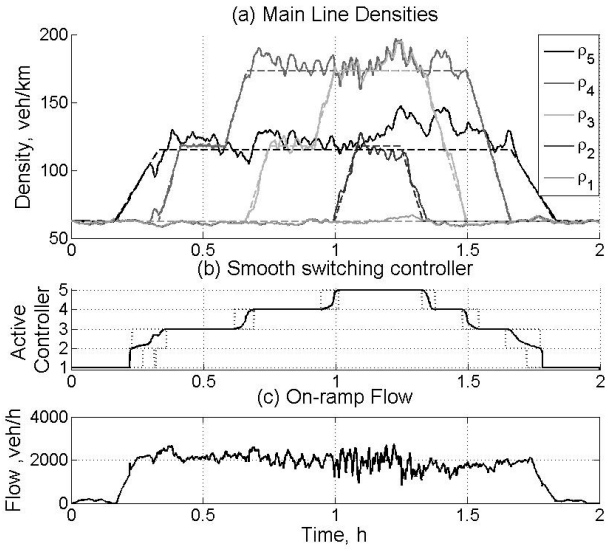

Fig. 10. Smooth Switching PI controller

may be conservative. As a future work, we can consider the relaxation of the LMI condition.

REFERENCES

C. F. Daganzo. The cell-transmission model, part 2: Network traffic. *Transportation Research Part B*, 29: 79–94, 1995.

Gang Feng. Controller synthesis of fuzzy dynamic systems based on piecewise lyapunov functions. *IEEE Trans. on Fuzzy Systems*, 11:605–612, 2003.

N. Geroliminis and C. F. Daganzo. Existence of urban-scale macroscopic fundamental diagram : Some experimental findings. *Transportation Research Part B*, (42): 759–770, 2008.

G. Gomes and R. Horowitz. Optimal freeway ramp metering using the asymetric cell transmition model. *Transportation Research Part C*, 14:244–262, 2006.

Habib Haj-Salem, Philippe Poirier, Jean-Franqois Heylliard, and Jean-Paul Peynaud. Alinea: a local traffic responsive strategy for ramp metering: Field results on a6 motorway in paris. In *IEEE Intelligent Transportation Systems Conference Proceedings*, pages 106–111, Oakland, USA, August 2001.

D Jacquet. Freeway traffic management using linear programming. *Proceedings of the 17th IFAC World Congress*, 2008.

D Jacquet, J Jaglin, D. Koenig, and C. Canudas De Wit. Non-local feedback ramp metering controller design. *Proceedings of the 11th IFAC Symposium on Control in Transportation Systems*, 2008.

Milael Johansson and Anders Rantzer. Computation of piecewise quadratic lyapunov function for hybrid systems. *IEEE Transaction on Automatic Control*, 43: 555–559, 1998.

Milael Johansson, Anders Rantzer, and Karl-Erik Arzen. Piecewise quadratic stability of fuzzy systems. *IEEE Trans. on Fuzzy Systems*, 7:713–722, 1999.

Milael Johansson, Anders Rantzer, and Karl-Erik Arzen. Piecewise linear quadratic optimal control. *IEEE Transaction on Automatic Control*, 45:629–637, 2000.

A. Kotsialos and M. Papageorgiou. A hierarchical ramp metering control scheme for freeway networks. In *Proceedings of the American Control Conference*, pages 2257–2262, Portland, June 2005.

Antoine Lemarchand, Damien Koenig, and John Jairo Martinez. Hierarchical coordinated freeway on-ramp metering using switching system theory. In *Proceedings of the Conference on Decision and Control*, Atlanta, Italy, December 2010a.

Antoine Lemarchand, John Jairo Martinez, and Damien Koenig. Hierarchical coordinated freeway on-ramp metering using switching system theory. In *IFAC Symposium on Structured System Control*, Ancona, Italy, September 2010b.

L. Munoz, X. Sun, D. Sun, G. Gomes, and R. Horowitz. Methodological calibration of the cell transmission model. In *Proceedings of the American Control Conference*, pages 798–803, Boston massachusetts, july 2004.

D. Schrank and T. Lomax. Mobility report. 2007.

Yorgos J. Stephanedes and Kai-Kuo Chang. Optimal control of freeway corridors. *ASCE Journal of Transportation Engineering*, 119:504–514, 1993.

X. Sun and R. Horowitz. A localized switching ramp-metering controller with a queue lenght regulator for congested freeways. In *Proceedings of the American Control Conference*, june 2005.

X. Sun and R. Horowitz. Set of new traffic-responsive ramp-metering algorithms and microscopic simulation results. *Journal of the Transportation Research Board*, 1959:9–18, 2006.